Int. J. Electrochem. Sci., 6 **(2011)** 181 -198

International Journal of
ELECTROCHEMICAL
SCIENCE
www.electrochemsci.org

Corrosion of Carbon Steel in Aqueous Carbonated Solution of MEA/ [bmim] [DCA]

Barham Hamah-Ali[*], *Brahim Si Ali, Rozita Yusoff, Mohamed Kheirodin Aroua*

Department of Chemical Engineering Faculty of Engineering
University Of Malaya 50603 Kuala Lumpur Malaysia
[*]E-mail: barham2007d@yahoo.com

Received: 12 December 2010 / *Accepted:* 30 December 2010 / *Published:* 30 January 2011

Carbon steel corrosion rates were measured in carbonated solution mixtures of monoethanolamine (MEA) and 1-Butyl-3-methylimidazolium dicyandiamide ([bmim] [DCA]) and MEA without [bmim] [DCA], using polarization curve and electrochemical impedance spectroscopy (EIS). Corrosion tests were carried out for 4.0 M carbonated MEA and [bmim] [DCA] concentration varied from 0.1 to 1.0 M. The CO_2 loading was 0.55 mol/mol and temperature was varied from 40 to 80 ^oC. Results showed adding [bmim] [DCA] decreased the corrosion rate of carbon steel for 4.0 M MEA/ [bmim] [DCA] system. However, the effect of [bmim] [DCA] addition was less as the temperature increased to 80 ^oC. Scanning Electron Microscope (SEM) and Energy dispersive X-ray analysis (EDX) were also carried out to characterize the surface morphology and corrosion product formed on the electrode surface. The SEM and EDX spectrum showed that a protective corrosion layer was formed on the electrode surface for 4.0 M MEA/ [bmim] [DCA] system. The corrosion rate of carbon steel was also measured using EIS at 40 ^oC and 4.0 M MEA/ 1.0 M [bmim] [DCA] with different exposure times. It was found the corrosion rate increased at first, but decreased progressively with time. The results from EIS are consistent with those found from the polarization curve, SEM and EDX.

Keywords: Carbon steel, CO_2 corrosion, MEA, ionic liquid, EIS

1. INTRODUCTION

CO_2 corrosion, usually called sweet corrosion, is one of the most serious forms of corrosion in oil and gas production and transport industries [1-3]. CO_2 dissociates in water to form carbonic acid (H_2CO_3), which is corrosive to carbon steel. According to Kohl and Riesenfeld [4], most of the equipment and piping in an alkanolamine plant is constructed of carbon steel. Alkanolamine solutions are commonly used to remove acid gases such as CO_2 from industrial flue gas to reduce the corrosion

rate of carbon steel caused by CO_2. Alkanolamine solutions are mainly classified into three types: primary, secondary and tertiary amines. Examples of these amines are monoethanolamine (MEA), diethanolamine (DEA), and N-methyldiethanolamine (MDEA) [5]. Among the alkanolamine solutions, MEA is considered more corrosive than other amines. Primary amines react with CO_2 to form more carbamate than secondary amine, while tertiary amines do not react with CO_2 directly [6]. It is well known, that $FeCO_3$ provides a passive barrier against more corrosion. For tertiary amines such as MDEA loaded with CO_2, a highly (or considerably) passive uniform layer of $FeCO_3$ will form and corrosion will be small even with high CO_2 loading. Alternatively, with primary and secondary amines or even mixtures of primary or secondary amines with tertiary amines, in CO_2 service, the passive $FeCO_3$ layer will not be uniform. In this case, the corrosion inhibitor is an important factor in to protect carbon steels [7]. Recently, ionic liquids based imidazolium have been used successfully as corrosion inhibitors on mild steel in acidic media such as HCl [8] and H_2SO_4 [9]. IL's have their unique properties such as negligible vapor pressure, non-flammability, high thermal stability, and high solvation capacity. These properties made ILs a good potential to replace conventional organic solvents of aqueous alkanolamine solutions [10]. Electrochemical impedance spectroscopy has been widely used to study the corrosion scale or to characterize the surface films formed on pure metals or alloys [11]. Farelas [12], showed the importance of EIS for getting the information about un-protective porous iron carbide layer, as well as precipitation of the protective iron carbonate inside the cementite layer.

The aim of this work is to find out the effect of ionic liquid based imidazolium on corrosion rate behavior of carbon steel in carbonated solution of 4.0 M MEA at temperature ranging from 40-80 ^oC, CO_2 loading 0.55 mol/mol and exposure time using EIS, polarization curves, SEM and EDX.

2. EXPERIMENTAL

2.1. Preparation of specimen and solutions

Monoethanolamine (MEA) with purity 99.5% and ionic liquid, 1-n-buty-3-methylimidazolium dicyandiamide ([bmim] [DCA]) with purity 98.0% were obtained from Fisher Scientific and Merck, respectively. The standard solutions, 1.0 M Hydroxide sodium (NaOH), 1.0 M Hydraulic acid (HCl) and $BaCl_2$ with purity 100% were also purchased from Merck. An aqueous solutions of 4.0M MEA, 4.0M MEA/ [bmim] [DCA], was prepared.

Carbon steel specimen of chemical composition (wt %) of C: 0.20%, Mn: 0.45%, P: 0.04%, S: 0.05%, Cr: 0.01 and Fe balance, was prepared to fit the specimen holder with a surface area (0.28 cm^2). Before each experiment the carbon steel specimen surface area exposed to the carbonated solution is polished with 600 and 2000 grit silicon carbide paper, then rinsed in acetone and washed with distill water.

An aqueous solutions of 2.0 M MEA, 4.0 M MEA, 2.0 M MEA/ [bmim] [DCA], and 4.0 M MEA/ [bmim] [DCA] were prepared. The test solution was prepared by purging a mixture of CO_2/N_2 or pure CO_2 to obtain the desired CO_2 loading. In this work, the test solution was loaded with 0.55 ±

0.05 mol of CO_2/mol of MEA or/and [bmim] [DCA]. The experiments were carried out at atmospheric pressure and at temperatures of 40, and 60 and 80 ^oC respectively. Prior to tests, the solution was deoxygenated by purging N_2 (99.95%) for 0.5 hours (h). Reaction of carbon dioxide with solution causes a decrease in alkalinity; Variation of pH solution was continuously recorded, when a constant pH was reach (solution is saturated with CO_2) the CO_2 loading were determined. To calculate the desired CO_2 loading, three samples (5 cm^3) were taken from saturated solution of MEA or/and MEA/ [bmim] [DCA] and mixed with an excess amount of (typically 50 cm^3) containing 1.0 M of $BaCl_2$ and 1.0 M NaOH and heated for three hours at temperature 70 ^oC and atmospheric pressure. After three hours of agitation, the samples were filtered to remove the fine white particle consist of Barium carbonate ($BaCO_3$) washed with distilled water to remove all traces of (NaOH), then titrated with 1.0 M of (HCl) using a PC controlled Metrohm 716 DMS autotitrator. The volume of (HCl) used to neutralize the basic species in the solution was determined from the end points which were automatically determined from the first derivative of the titration curve.

The CO_2 loading, α, was calculated according to the following equation [5]:

$$\alpha = \frac{V_{HCl}}{V_{sample} \times 2 \times M} \qquad (1)$$

Where,

α: CO_2 loading in mol of CO_2/mol of solution.

V_{HCl}: Volume of HCl request to neutralized the $BaCO_3$ in cm^3.

V_{sample}: Volume of sample taken for analysis in cm^3.

M: The molarity of the solution in mol/l.

2.2 *Electrochemical Setup*

Fig.1 illustrates the electrochemical setup used in this work. It consists of the corrosion cell with capacity of 100 cm^3 and Potentiostat/Galvanostat /ZRA (REF 600) model and a Radiometer with a speed controller (FCTV101) model and a data-acquisition system. Three electrodes system was used, a platinum wire as counter electrode (auxiliary electrode), working electrode (specimen) and a calomel-saturated electrode (CSE) as reference electrode. The working electrode was subjected to a constant rotation speed of 600 rpm via a radiometer speed control unit.

The temperature of the solutions was controlled using water bath with accuracy ±0.1 ^oC. The gases (CO_2 and N_2) flow rates were regulated using brooks gas mass flow meters model (5850E) for N_2 and (5850C) for CO_2 and controlled by a four channel brooks mass flow controller model (0154E).

A water-cooled condenser was used to prevent any change in solution concentration due to water evaporation. A computer controlled Potentiostat was used for corrosion measurement. The experiments were monitored using the software Echem Analyst 5.6 Software.

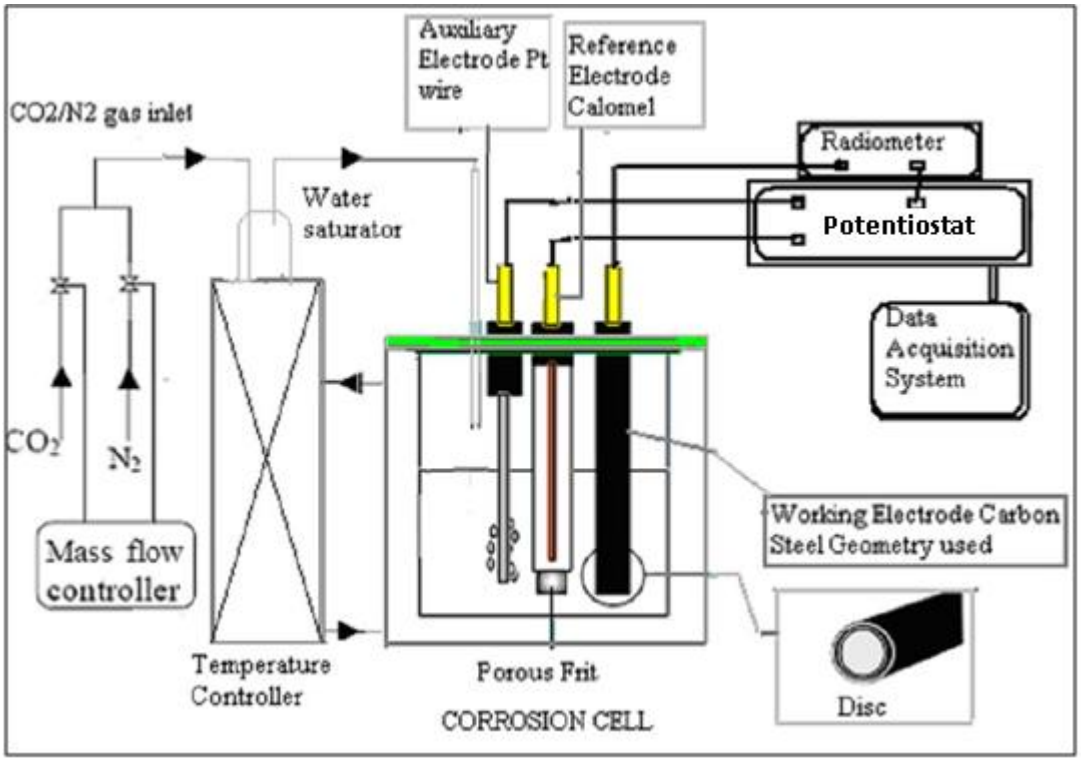

Figure 1. Shows the electrochemical experimental set-up for corrosion experiment. [15].

2.3 Electrochemical procedure

The electrochemical corrosion tests were carried out according to ASTM G5-94 [18] to ensure the electrochemical data obtained are reliable by conducting the anodic polarisation curve on a stainless steel-430 specimen in a 0.5 M sulfuric acid (H_2SO_4) solution at 30 °C. Before polarization experiment, the open circuit potential (OCP) measurements were taken until the stability was reached. Potentio-dynamic polarization curves were then obtained at 0.9 mV/sec scanning rates covering a potential range of 500 mV around the free corrosion potential. The corrosion rate was determined later using Tafel extrapolation method.

This method estimates the corrosion current density I_{corr} ($\mu A/cm^2$) which can be converted to corrosion rate by using equation (2).

$$CR = \frac{0.00327 \times I_{corr} \times W}{n \times D} \qquad (2)$$

Where; CR: is the corrosion rate in $(\mathbf{mm\ year^{-1}})$, W: is the atomic weight of specimen in (55.85 gm/mol), n: is the number of electrons transferred in the corrosion reaction (n= 2) and D: is the density of the specimen in (7.88 gm/cm^3).

EIS measurements were carried out using AC signals, of which the amplitude of input sine wave voltage was 5 mV and the range of frequency was varied from 0.1 Hz to 100 kHz. All impedance data were fitted to appropriate equivalent circuits (EC) using the Gamry Echem Analyst software. Potentio-dynamic polarization curves were then obtained at 0.9 mV/sec scanning rates covering a potential range of $500\ mV$ around the free corrosion potential. At the end of each experiment, the conductivity values were determined using Fisher scientific conductivity-meter (accuracy$\mp 0.1\ \mu S/cm$).

Surface morphology and characteristic analyzed using Scanning Electron Microscope (SEM) and Energy-dispersive X-ray spectroscopy (EDX), in high vacuum condition.

3. RESULTS AND DISCUSSION

3.1. Polarization Curve

3.1.1. Effect of [bmim][DCA] Concentration in 4.0M MEA

Figure 2 shows the polarization curves of carbon steel in a carbonated solution of 4.0 M MEA with and without [bmim] [DCA] at CO_2 loading of 0.55 mol/mol and a temperature of 40 ^oC. In the presence of [bmim] [DCA], the corrosion potential shifted towards the positive (noble) directions and caused a decrease in corrosion rate. This large shift to noble directions suggests that the [bmim] [DCA] blocked the active site on the surface of carbon steel and has acted as a barrier for oxidizer species. Adding [bmim] [DCA] did not substantially change the polarization behavior from those of 4.0 MEA alone. But the addition of [bmim] [DCA] decreases both the anodic and cathodic currents.

The Figure also provides information on corrosion behavior under a passivation condition between -0.55 and -0.35 (V Vs. SCE). It is clear that the passivation current densities decreases with increasing [bmim] [DCA] concentrations, which suggests the passive layer on the surface of carbon steel is strengthened in the presence of [bmim] [DCA] due to block the active sites on the electrode surface.

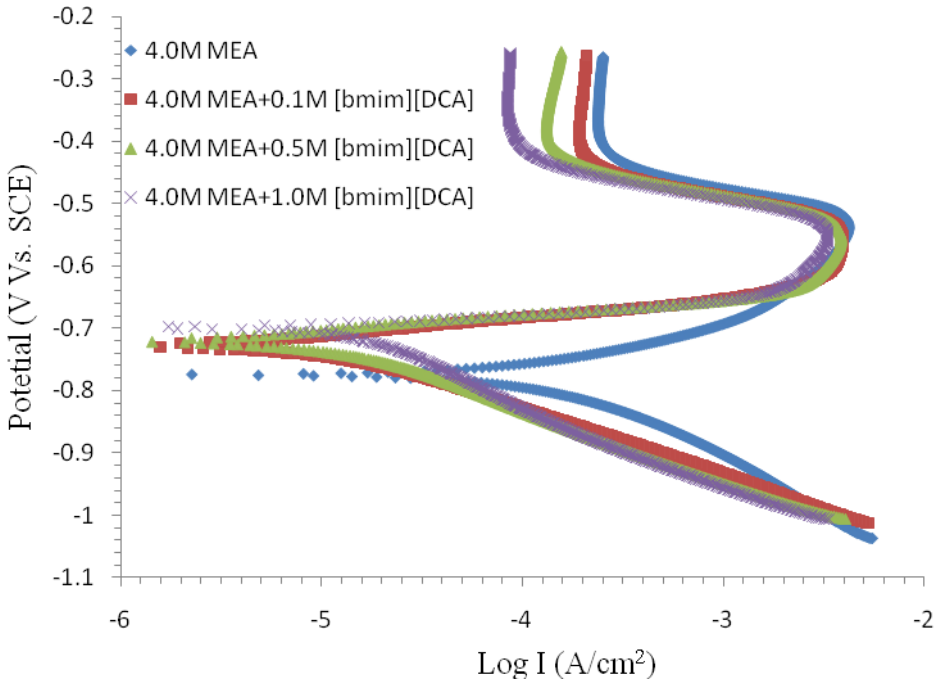

Figure 2. Effect of [bmim] [DCA] Concentrations on Polarization Curve in 4.0 M MEA Solution at 40 ^{o}C and CO_2 loading of 0.55 mol/mol

Table (1) presents the summary of conductivity and the parameters were extracted from the polarization curves of 4.0 M MEA/ [bmim] [DCA] at CO_2 loading of 0.55 mol/mol and 40 ^{o}C. It is observed that the solution conductivity decreases with increasing [bmim] [DCA] concentration and the corrosion rate of carbon steel decreased.

Also it can be seen that the corrosion rate decreased considerably with increasing [bmim] [DCA] concentration. The anodic Tafel slope (b_a) and cathodic Tafel slop (b_c) of 4.0 M MEA/[bmim] [DCA] decreased with [bmim] [DCA] concentration, indicating that the [bmim] [DCA] controlled both the reactions.

Table 1. Summary of the parameters extracted from the polarization curve of 4.0 M MEA and 4.0M MEA/ [bmim] [DCA] at CO_2 loading of 0.55mol/mol and temperature 40 ^{o}C.

4.0MMEA+ [bmim] [DCA] (M)	T (^{o}C)	Conductivity K (S/cm)	b_a mV/dec	b_c mV/dec.	E_{corr} mV	I_{corr} µA/cm^2	CR mm year^{-1}
0	40	48.7	110	170	-774	165.0	1.914
0.1	40	45.2	37	112	-728	15.25	0.177
0.5	40	39.4	32	130	-719	13.80	0.160
1.0	40	34.4	28	130	-699	10.00	0.116

3.1.2. Effect of temperature

The effect of solution temperature (Figure 3) in carbonated solution of 4.0 M MEA+ 1.0 M [bmim] [DCA] discussed at CO_2 loading of 0.55 mol/mol.

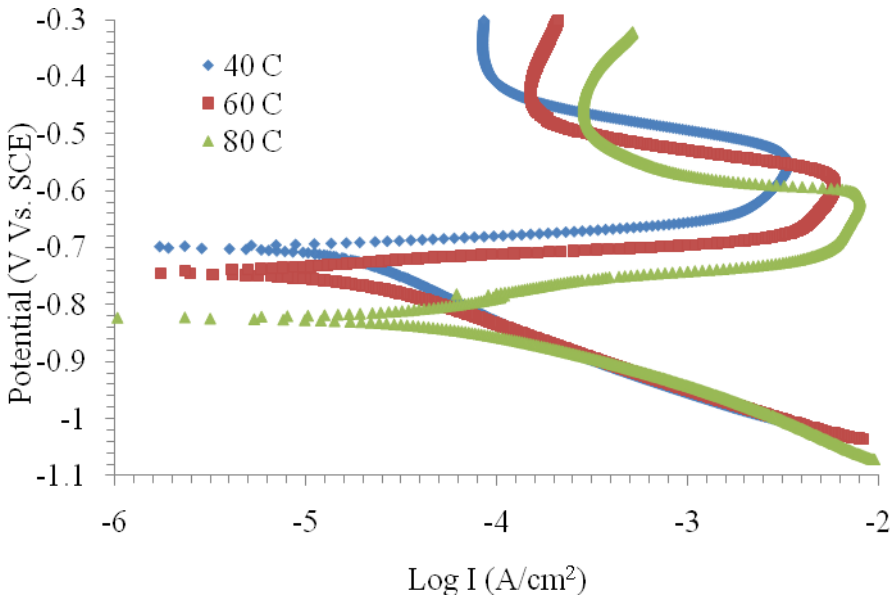

Figure 3. Effect of solution temperature on Polarization Curve in 4.0 M MEA/ 0.1 M [bmim] [DCA] Concentrations at CO_2 loading of 0.55 mol/mol.

It is noted that the increase in solution temperature has a great impact on corrosion rate of carbon steel. As temperature was increased from 40 ^oC to 80 ^oC, the corrosion potential shifted towards active directions and caused an increase in corrosion rate. This might be due to desorb [bmim] [DCA] on the electrode surface which results in more active sites to be available for cathodic reactions. The increase in solution temperatures markedly increases the anodic reaction, while the cathodic reaction remains unchanged. This attributed to the high rates of iron dissolution which is evidenced by the higher anodic current density.

As shown in Figure 2, the passivation current density (I_p) increased with increasing temperature suggesting that the passive layer formed on the surface of carbon steel detected or damaged with temperature and caused the corrosion rate to increase.

Table 2. Summary of the parameters extracted from the polarization curves of 4.0 M MEA and 4.0 M MEA+1.0 M [bmim] [DCA] at CO_2 loading of 0.55 mol/mol and different temperatures.

4.0M MEA+ [bmim] [DCA] (M)	T (^oC)	Conductivity K (S/cm)	B_a mV/dec	B_c mV/dec.	E_{corr} mV	I_{corr} µA/cm^2	CR mmyear^{-1}
0	40	48.7	107.6	160.3	-774	156.0	1.914
	60	45.1	42.8	120.6	-776	188.6	2.188
	80	41.5	134.4	116.4	-862	274.0	3.174
1.0	40	34.4	28.00	130.0	-699	10.00	0.116
	60	33.4	30.00	120.0	-746	18.62	0.216
	80	34.9	56.00	118.0	-789	88.80	1.030

Table (2) presents the summary of conductivity and the parameters extracted from the polarization curves of 4.0 M MEA and 4.0 M MEA+ 1.0 M [bmim] [DCA]. It is found that the solution conductivity increased with temperature. This might be due to increase the ionic concentration of the solution taking place with iron dissolution. This Table also shows that in absence of [bmim] [DCA] the corrosion rate increased rapidly and reaches a maximum value of around 3.174 mm $year^{-1}$. On addition of [bmim] [DCA], the corrosion rate decreased dramatically due to decreased the CO_2 reaction between the electrode and bulk solution.

3.2. EIS Study

3.2.1. Effect of [bmim] [DCA] Concentration in 4.0 M MEA

EIS technique has the advantage of rapid determination of corrosion rate and the ability to provide information on the film formation on the surface of the specimen (carbon steel). Figure 4 presents the Nyquist plots of carbon steel in carbonated solution of 4.0 M MEA with and without [bmim] [DCA].

Without [bmim] [DCA], the Nyquist plot showed two capacitive loops at high and low frequencies, respectively. At carbonated 4.0 M MEA-[bmim] [DCA], the Nyquist plots exhibited with a capacitive loop and an inductive loop at low frequency, which is associated to adsorption of intermediate products on the carbon steel surface [12]. This means that the corrosion mechanism changed on the carbon steel surface when carbon steel exposure to carbonate of MEA-[bmim] [BF_4].

As Figure 4 shows, the semicircle of Nyquist plots increased with the addition of [bmim] [DCA] indicating the resistance to charge transfer increased, which suggests the [bmim] [DCA] induced inhibition against the CO_2 corrosion of carbon steel. In other words, the increase in semicircle of Nyquist plots has been identified by reducing both the anodic and cathodic current densities in polarization curve Figure 2. Further analysis has been performed on the surface of carbon steel to characterize the surface film using SEM and EDX (see Figures 5 and 6) respectively. The SEM images obtained after immersing the tested sample for 168 hours in carbonated solution of 4.0 M MEA with and without [bmim] [DCA] at 40 ^oC and CO_2 loading 0.55 mol/mol. In absence of [bmim] [DCA], as expected a rough surface to be covered with non-uniform corrosion products Figure 9a. In contrast, in appearance of [bmim] [DCA], the metallic surface is almost no affected by corrosion. In other words, the surface covered with a thick layer and improved with increasing [bmim] [DCA] concentration. The EDX as shown in Figure (10) showed that adding 0.5 M of [bmim] [DCA] to 4.0 M MEA caused a decrease in Fe peak compared to the blank sample (4.0 M MEA). This means the surface of carbon steel covering with a barrier of the film. These results confirm those from polarization and EIS measurements, which suggested the corrosion rate of carbon steel decreased with increasing [bmim] [DCA] concentrations.

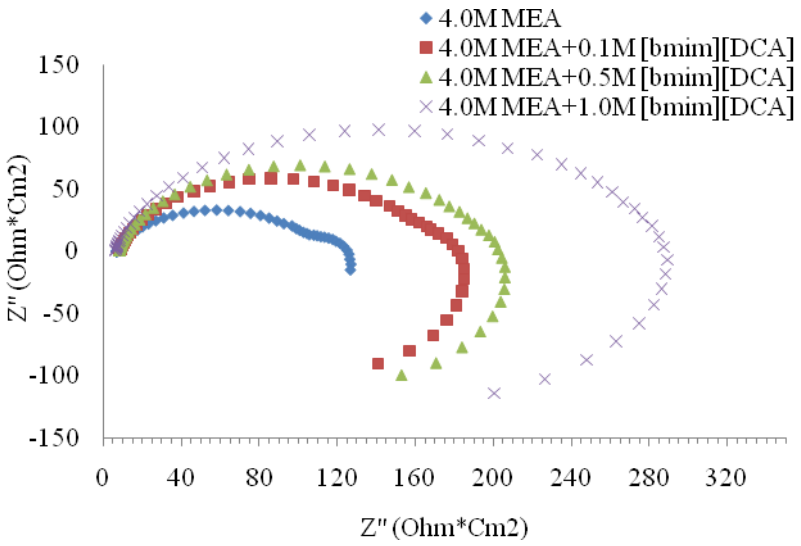

Figure 4. Nyquist plots of carbon steel in 4.0M MEA /[bmim] [DCA] at 40^{o}C and CO_2 loading of 0.55mol/mol.

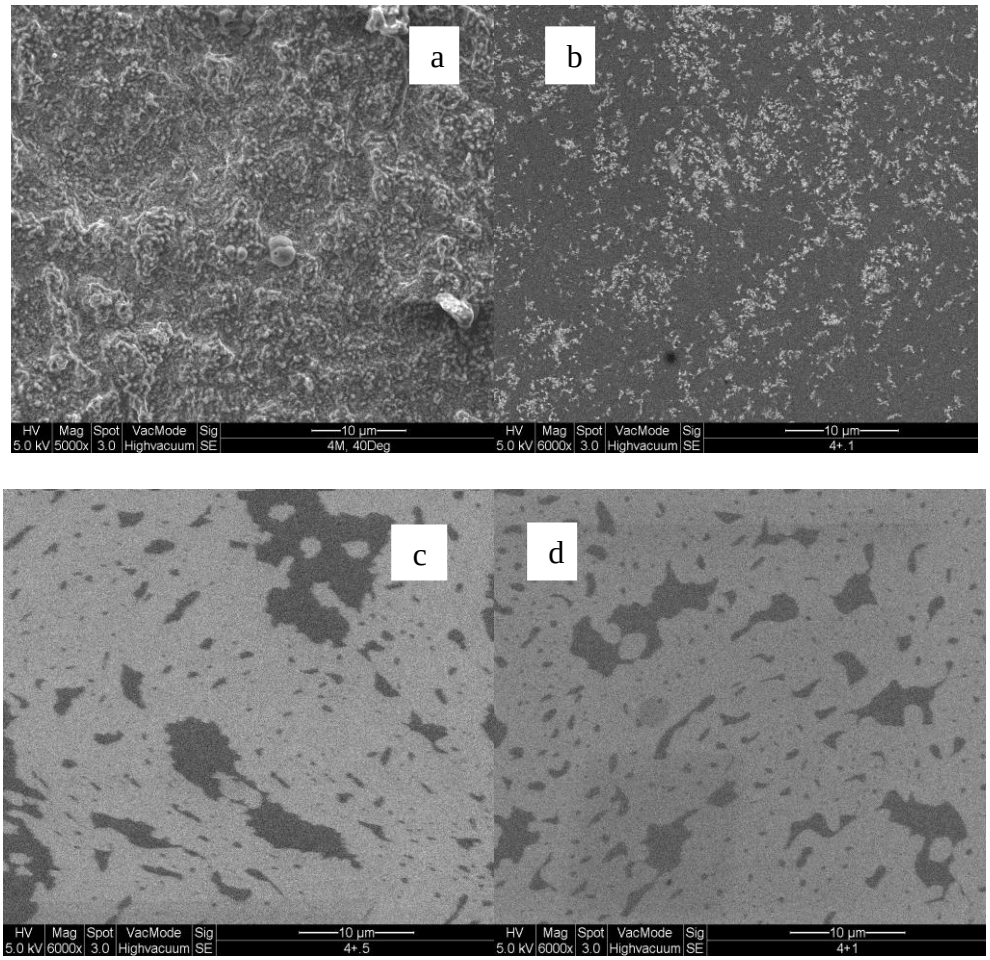

Figure 5. SEM images for carbon steel in carbonated solution of: a. 4.0 M MEA b. 4.0 M MEA+0.1 M [bmim] [DCA c. 4.0 M MEA+0.5 M [bmim] [DCA] d. 4.0 M MEA+1.0 M [bmim] [DCA].

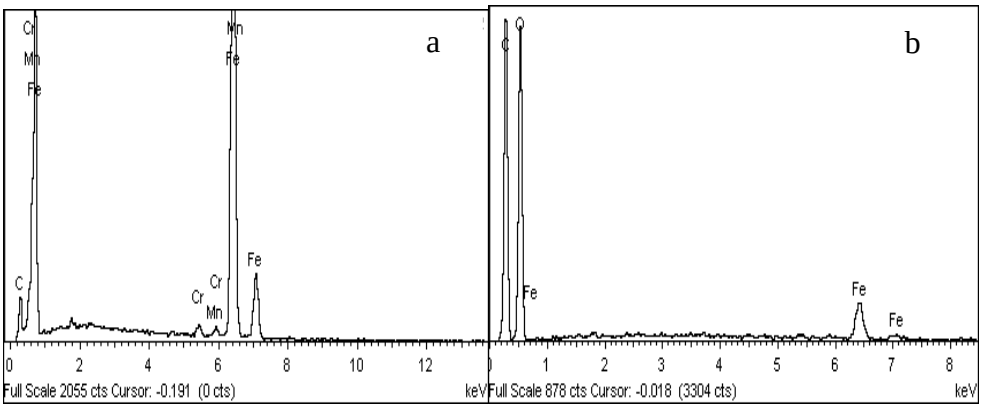

Figure 6. EDX analysis carbon steel in carbonated solution of: a. 4.0 M MEA b. 4.0 M MEA+0.5 M [bmim] [DCA].

Its corresponding Bode plots (Figure 7) shows the presence of [bmim] [DCA] results in an increase in the impedance when compared to that obtained without [bmim] [DCA]. Another aspect is Bode phase angle diagrams presented in Figure (8) shows that the phase angle increased with increasing [bmim] [DCA] concentrations. This might be contributed to form a resistive layer on the carbon steel surface. Figure 8 also provides information on capacitive behaviour. The increase in [bmim] [DCA] leads to shift the phase angle to a more capacitive behavior due to continuous imidazolium stepped on the surface [7].

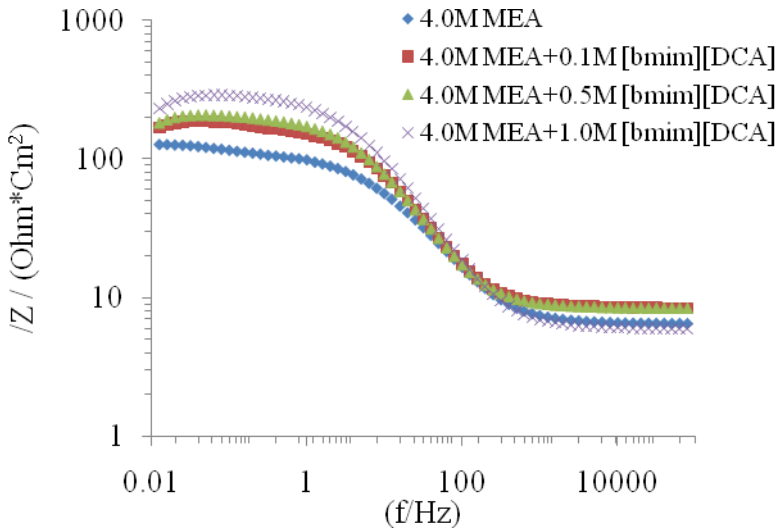

Figure 7. Bode plots of carbon steel in 4.0 M MEA /[bmim] [DCA] at 40 ^{o}C and CO_2 loading of 0.55 mol/mol.

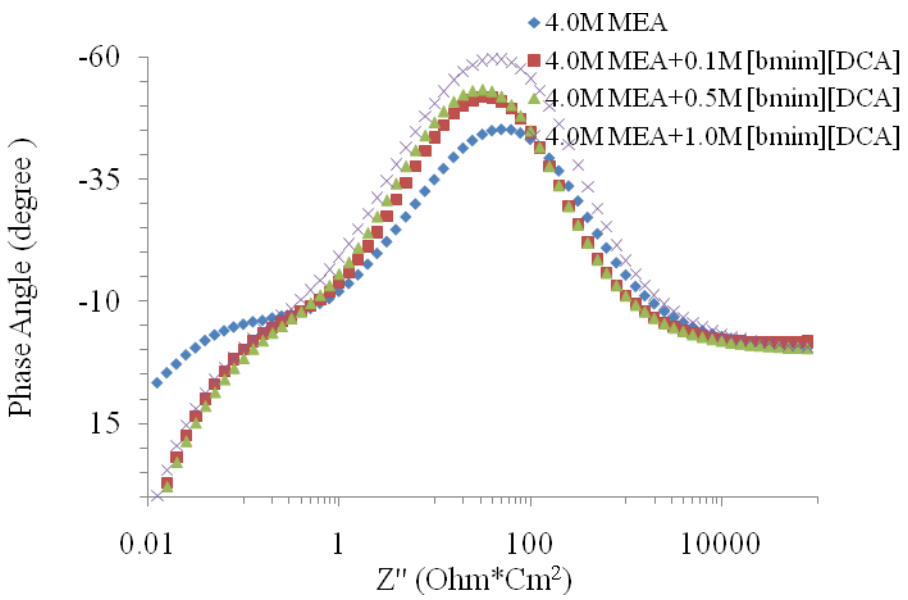

Figure 8. Phase angle plots of carbon steel in 4.0 M MEA /[bmim] [DCA] at 40^{o}C sand CO_2 loading of 0.55 mol/mol.

Figure 9 (a and b), represents the equivalent circuits that were used to model the system under investigation. The parameters of interests such as electrolyte resistance (R_s), double layer capacitance (Q_{dl}), pores layer capacitance (Q_{po}), charge transfer resistance (R_{ct}), and pore resistance (R_{po}), inductive resistance (R_L) and inductance (L) can be obtained from the equivalent circuits. The behavior of the double layer formed on the surface of the specimen, is equivalent to a capacitor. However, it cannot be modeled as an ideal capacitor, just because the behavior is not exactly as a capacitor. Nonetheless, a constant phase element (CPE) is used instead. CPE impedance is calculated using the following equation

$$Z_{CPE}=1/\ Q\ (jw)^{a} \quad \text{.....(3)}$$

Where Z_{CPE} is the impedance of CPE, Q is a proportional factor (CPE), j is $\sqrt{-1}$, w is $2\pi f$, and a is a factor which takes a value between 0 and 1. Nyquist plots fitted to the equivalent circuit represented in Figure 9 (a and b), and the parameters extracted from the model summarized in Table 3.

Table (3) Summary of the parameters extracted from the EIS method for 4.0 MMEA/ [bmim] [DCA] at CO_2 loading of 0.55 mol/mol and temperatures 40 °C.

4.0 MEA+[bmim] [BF4]	0.0	0.1	0.5	1.0
R_s (Ohm*cm^2)	6.205	8.972	8.319	5.609
Q_{po} (F.s^(a-1)/cm^2)	0.000616	0.000351	-	-
R_{po}(Ohm*cm^2)	103.5	153.8	-	-
Q_{dl} (F.s^(a-1)/cm^2)	0.064	0.00421	0.000436	0.000390
a	0.743	0.770	0.797	0.8
R_{ct} (Ohm*cm^2)	14.27	30	192.6	290.3

A good fit with this model existed with our experimental data as shown in Fig. (8). It can be seen that the charge transfer resistance (R_{ct}) values for the carbon steel in carbonated of 4.0 M MEA+ [bmim] [DCA] are higher than that of 4.0 M MEA alone. This indicates that the corrosion rate decreased due to less active site available for charge transfer. In contrast, the capacitance values (Q_{dl}) tend to decrease with the introduction of [bmim] [DCA]. This can be attributed to a decrease in the dielectric constant and/or an increase in the double electric layer thickness due to [bmim] [DCA] adsorption or stepped on the metal/electrolyte interface [13].

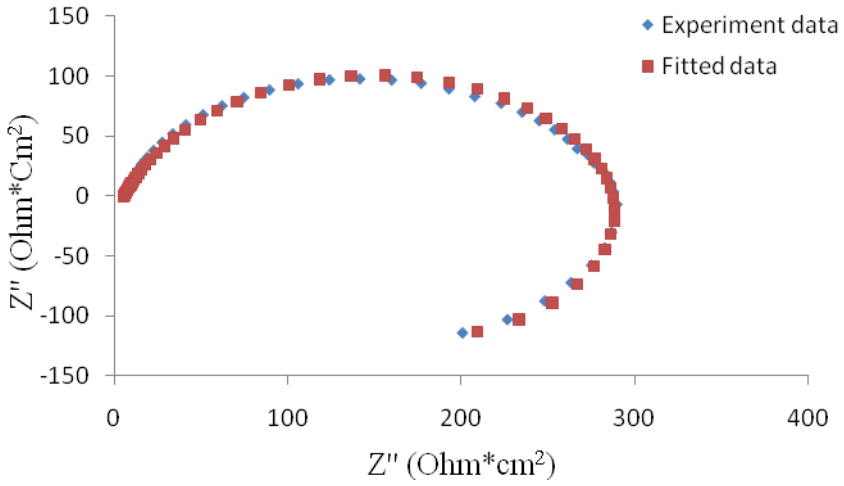

Figure 8. Nyquist plots of carbon steel in 4.0 M MEA and 1.0 M [bmim] [DCA] at 40°C and CO_2 loading of 0.55 mol/mol.

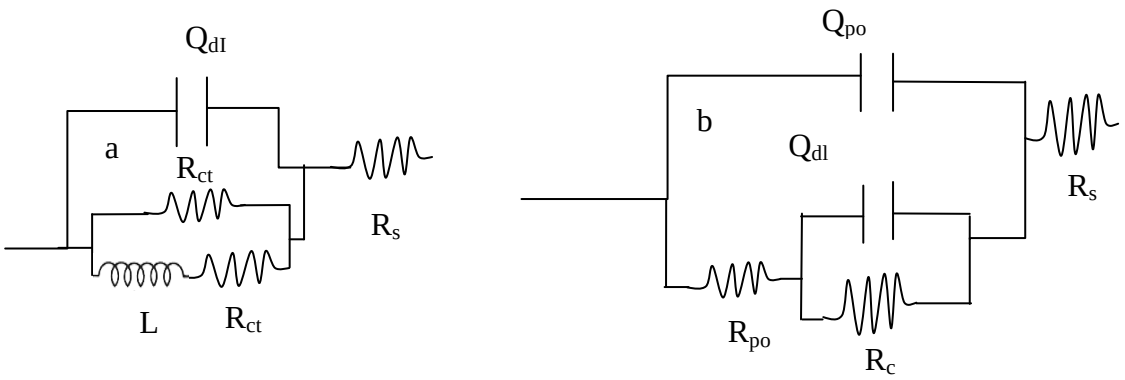

Figure 9. (a and b) Equivalent circuits used to fit the EIS data earned for carbon steel in solutions of 4.0 M MEA and [bmim] [DCA].

3.2.2. Effect of temperature

Figures (11-13) present typical Nyquist plots and its equivalent Bode plots. These plots generated using EIS measurements, for the carbonated solutions of 4.0 M MEA+1.0 M [bmim] [DCA] concentrations at temperatures ranged from 40 to 80 ^{o}C and loading of 0.55 mol/mol. As the temperature was increased from 40 to 80 ^{o}C, the diameter of Nyquist plots decreased and caused an increase in corrosion rate. An interpretation of this behaviour stated that increasing the temperature results in desorption of the imidazolium from the surface of the electrode [17].

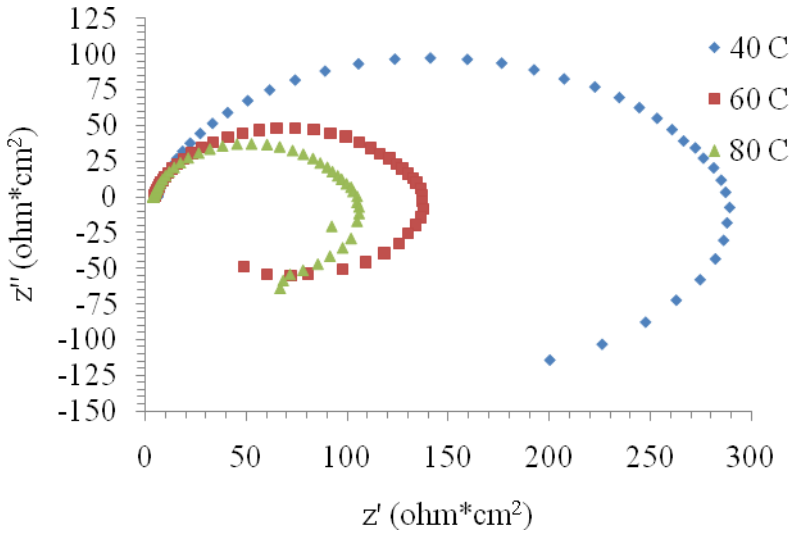

Figure (11), Effect of temperature on Nyquist plots of carbon steel in 4.0 M MEA +1.0 M [bmim] [DCA] at CO_2 loading of 0.55 mol/mol.

Figure 12 shows Bode plots for the same conditions mentioned above. It can be seen that increasing the temperature results in decrease in the impedance /Z/ of the electrode. On the other hand, the phase angle plots at HF frequency Figure 13, shows the characteristic charge transfer process due to dissolution process [12].

It is noted that the phase angle at low temperatures was picked at high values and then decreased with increasing solution temperatures. This implies that the corrosion rate increased. This result was in good agreement with that found in polarization curves shown in Figure 3.

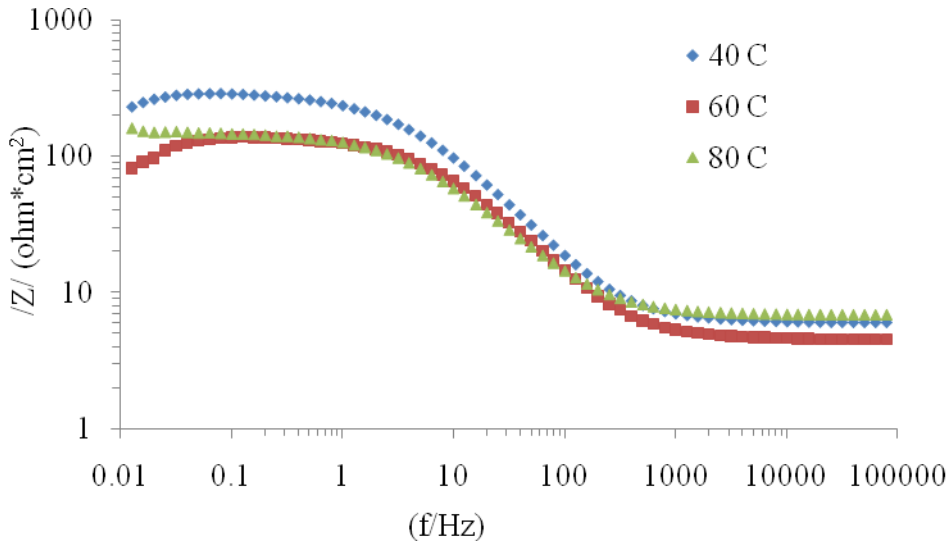

Figure 12. Effect of temperature on phase angle of carbon steel in 4.0 M MEA+1.0 M [bmim] [DCA] at CO_2 loading of 0.55 mol/mol.

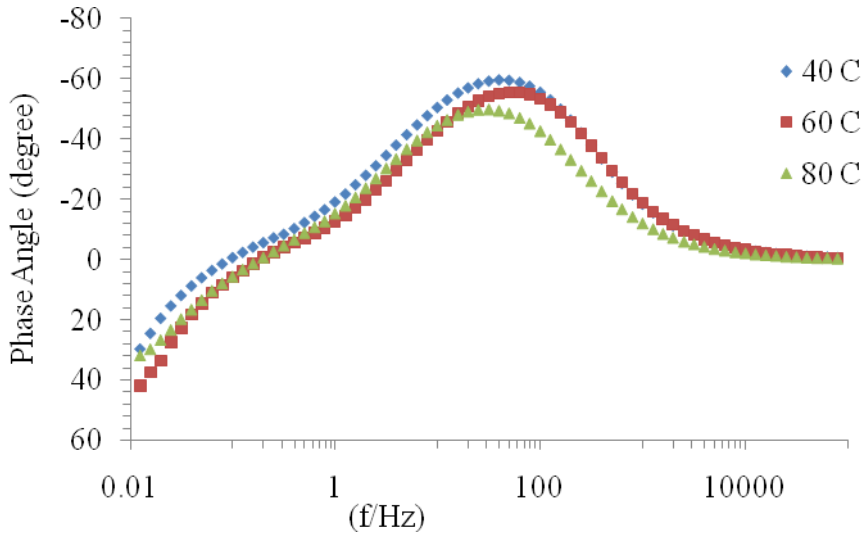

Figure 13. Effect of temperature on bode of carbon steel in 4.0 M MEA+1.0 M [bmim] [DCA], at CO_2 loading of 0.55 mol/mol

Table (4) shows the parameters which were evaluated from the Nyquist plots for 4.0 M MEA with and without [bmim] [DCA] at different temperatures and at CO_2 loading of 0.55 mol/mol. It is observed that the R_s decreased with increasing solution temperature which indicates an acceleration of corrosion rate. In presence of [bmim] [DCA], the Q_{Id} values tend to increase with temperature.

This suggests that the nature of the layer of products formed on the electrode surface is modified by [bmim] [DCA]. This Table also shows that in absence of [bmim] [DCA] the charge transfer markedly decreased to 7.0 (Ohm*cm^2) at 80 ^{o}C. On addition of 1.0 M [bmim] [DCA], the charge transfer increased from 7.0 to 95.39 (Ohm*cm^2) at the same temperature, due to decreased the CO_2 reaction between the electrode and bulk solution.

Table (4) Summary of the parameters extracted from the EIS method for 4.0 MMEA/ [bmim] [DCA] at CO_2 loading of 0.55 mol/mol and different temperatures 40-80 ^{o}C.

4.0 MEA+[bmim] [DCA]	Temperature (^{o}C)	R_s (Ohm*cm^2)	Q_{dl} (F.s^(a-1)/cm^2)	a	R_{ct} (Ohm*cm^2)
0.0	40	6.205	0.064000	0.743	14.27
	60	3.298	0.031600	0.774	13.00
	80	3.670	0.025000	0.761	07.00
1.0	40	5.609	0.000390	0.773	290.3
	60	4.228	0.000587	0.742	141.3
	80	3.944	0.000469	0.688	95.39

4. Effect of exposure time for optimum 4.0 M MEA+1.0 M [bmim][DCA]

Impedance spectrum was measured at different immersion times up to 24 h of immersion, without removing the working electrode between measurements. In Figure (14), the Nyquist plot is presented for 4.0 MEA+1.0 [bmim] [DCA] system at different exposure times at 40 ^{o}C and CO_2 loading of 0.55 mol/mol.

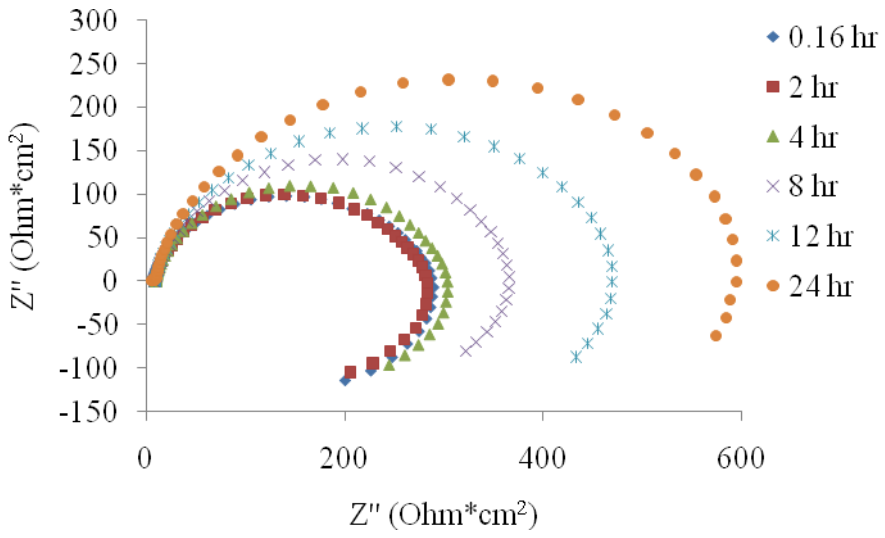

Figure 14. Effect of time on Nyquist plots of carbon steel in 4.0 M MEA /1.0[bmim] [DCA] at 40 ^{o}C and CO_2 loading of 0.55 mol/mol.

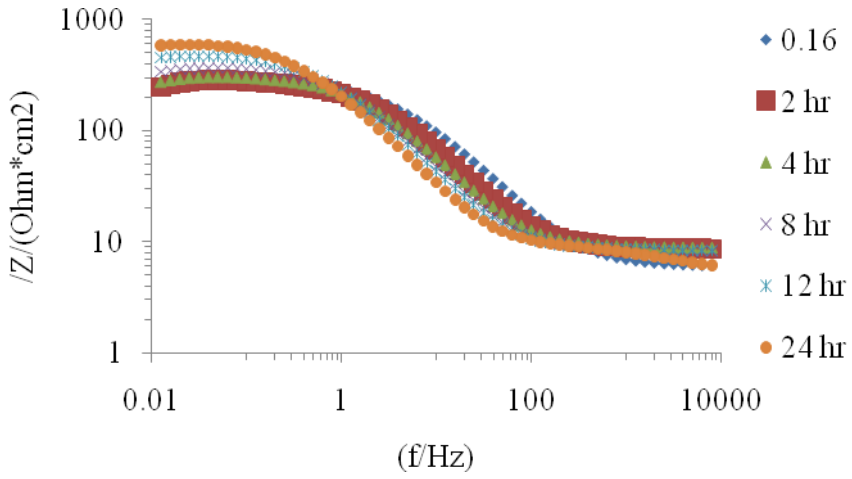

Figure 15. Effect of time on phase angle plots of carbon steel in 4.0 M MEA /1.0 [bmim] [DCA] at 40 ^{o}C and CO_2 loading of 0.55 mol/mol.

It is observed the diameter of Nyquist plot decreased with increasing the exposure time to 2 h. While the exposure time exceeds 2 h, the diameter of Nyquist plots increase. This is attributed to form a thick film and continuously growth on the surface. An increase in the exposure time resulted in decreasing of the capacitive loop. This might be because of accumulation of $FeCO_3$ and [bmim] [DCA] molecules on the surface. Bode plots presented in Figure (15) which shows the impedance of the electrode increased with increasing exposure time. Furthermore, the phase angle plots Figure (16), shows that all plots have peaks at high frequency and these peaks increased gradually with exposure time.

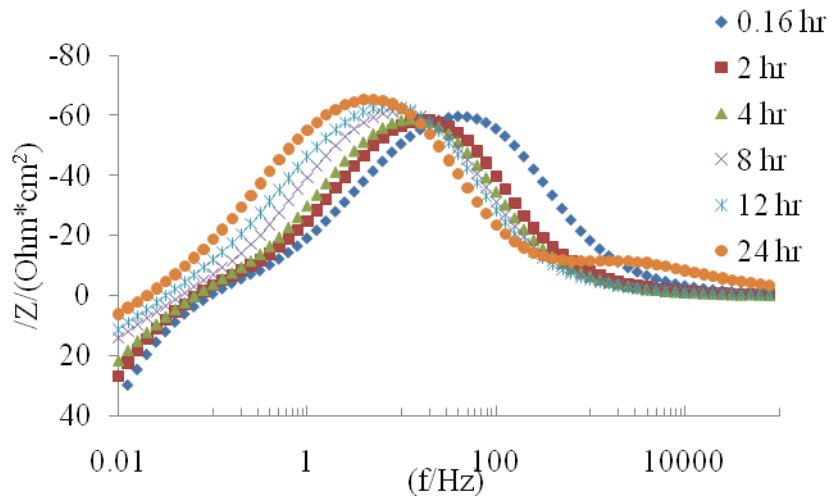

Figure 16. Effect of time on Bode plots of carbon steel in 4.0 M MEA /1.0 [bmim] [DCA] at 40 ^{o}C and CO_2 loading of 0.55 mol/mol.

The same electrical equivalent circuits were used as mentioned previously, Figure (9a). Table (5) shows the parameters evaluated from the Nyquist plots for 4.0 MEA + 1.0M [bmim] [DCA] at different times and CO_2 loading of 0.55 mol/mol. It is observed the charge transfer resistance (R_{ct}) between the electrode and solution was larger than the first immersion time at 2 h. This can be ascribed to form the protective surface film on the electrode and its continuous growth with exposure time due to reduce uncovered area available for charge transfer [14]. It is also noted that the Q_{Id} values increase with increasing the exposure time. This is attributed to the growing area of an iron carbonated on the surface of electrods [16].

Table 5. Summary of the parameters extracted from the EIS method for 4.0 MMEA/ 1.0 [bmim] [DCA] at different exposure time and CO_2 loading of 0.55 mol/mol, and temperatures 40 °C.

4.0 MEA+1.0 [bmim] [BF_4]	0.16 hr	2 hr	4 hr	8 hr	12 hr	24 hr
Rs (Ohm*cm^2)	5.609	8.441	8.884	8.219	8.256	6.344
Q_{dI} (F.s^(a-1)/cm^2)	0.390	0.498	0.537	0.638	0.749	0.991
a	0.8	0.826 2	0.849 7	0.860 4	0.848	0.819
Rct (Ohm*cm^2)	290.3	276.1	293.2	359.4	469.2	634.9

5. CONCLUSIONS

Our study reports the effects of 1-Butyl-3-methylimidazolium dicyandiamide ([bmim] [DCA]) in carbonated solution of 4.0 M using polarization curve, EIS measurements and SEM–EDX investigations. In this work also the effect of exposure time was studied.

Polarization technique showed the [bmim] [DCA] acted as mixed-type by decreasing both reactions anodic and cathodic. Addition of [bmim] [DCA] to 4.0 M MEA solution decreased the corrosion rate without change the mechanism of reactions. Impedance technique also pointed to the presence of [bmim] [DCA] raises both the surface and the charge transfer resistances, but decreases with the increase of temperature. In general, the data gained from both techniques EIS and polarization curve were in a good agreement.

SEM and EDX examinations of the MEA alone and MEA+ [bmim] [DCA] revealed the presence of a protective film on the electrode surface. The EIS data shows that the charge transfer increased with increasing the exposure time, except for the first time where the R_{ct} was decreased.

ACKNOWLEDGMENT
This work was financially supported by University of Malaya through the High Impact Research Grant No. VC/HIR/001, PPP grant No.PS111/2009B, and PJP grant No.FS225/2008A.

References

1. X. Zhang, F. Wang, Y. He, & Y. Du. *Corr. Sci.*, 43 (2001) 1417-1431.
2. A. Dugsted, L. Lunde, S. Nesic. *Gulf Publishing Co*, 1994.
3. S. Nesic, B.F.M. Pots, J. Postlethwaite, N. Thevenot, *Corr. Sci. Eng*. 1 (1996) paper 3.
4. A.L Kohl, R. B. Nielson, Gas Purification, 5th ed.; Gulf Publication Co. Houston, TX, 1997.
5. A. benamor, M.K. Aroua. *Fluid Phs. Eq*. 231 (2005) 150-162.
6. X. P. Guo, Y. Tomoe. *Corros. Sci.*, 41(1999), 1391-1402.
7. F. Farelas, A. Ramirez. *Int. J. Electrochem. Sci*. 5 (2010) 797 – 814
8. Q.B. Zhang, Y.X. Hua. *Electrochim. Acta*, 54 (2009) 1881–1887.
9. V. L. Natalya, A. D. Marco, Octavio Olivares-Xometl, Noel Nava-Entzana, Elsa Arce, Hector Dorantes. *Corros. Sci*. 52 (2010) 2088–2097.
10. N. S. Allan, T. D. Bonifacio, Hui. Meng, *J. Chem. Therm*., 41(2009) 525-529.
11. S.L. Wu, Z.D. Cui, G.X. Zhao, M.L. Yan, S.L. Zhu, X.J. Yang. *App. Sur. Sci*., 228 (2004) 17–25.
12. F. Farelas, M. Galicia, B. Brown, S. Nesic, H. Castaneda. *Corros. Sci*., 52 (2010) 509–517.
13. P.C. Okafor a,b, X. Liu a,c, Y.G. Zheng. *Corros. Sci*. 51 (2009) 761–768.
14. J. Mar´ın-Cruz a,b, R. Cabrera-Sierra a,c, M.A. Pech-Canul d, I. Gonz´alez. *Electrochim. Acta* 51 (2006) 1847–1854
15. B. S. Ali, PhD Thesis. University of Malaya (2005).
16. D. A. Lo´pez , S.N. Simison, S.R. de Sa´nchez. *Electrochim. Acta*, 48 (2003) 845-854.
17. Q.B. Zhang, Y.X. Hua. *Electrochim. Acta*, 54 (2009) 1881–1887.
18. ASTM Standard G5-94 (Reapproved 1999), ASTM: Philadelphia, PA, 1999.